

# Characterization of Quiescent Epithelial Cells in Mouse Meibomian Glands and Hair Follicle/Sebaceous Glands by Immunofluorescence Tomography

*Journal of Investigative Dermatology* (2015) 135, 1175–1177; doi:10.1038/jid.2014.484; published online 18 December 2014

## TO THE EDITOR

As epithelial appendages of the skin, hair follicle/sebaceous glands (HF/SGs) and eyelid meibomian glands (MGs) are developmentally similar and share common characteristics including holocrine differentiation, lipid secretion, and the need for long-term proliferative capacity and self-renewal (Knop *et al.*, 2011). Although the capacity for self-renewal has been linked to the presence of a quiescent adult stem cell pool in the epidermis (Tumbar *et al.*, 2004), cornea (Cotsarelis *et al.*, 1989), and intestine (Pinto and Clevers, 2005), the location and characterization of MG and SG stem cells remain controversial. To address this problem, we used a novel three-dimensional (3D) reconstruction technique, immunofluorescence tomography, to identify label-retaining cells (LRCs) using the H2B-GFP/K5tTA 'tet-off' mouse model (Tumbar *et al.*, 2004) and further characterize LRCs based on expression of SOX9 and BLIMP1.

Eyelids from three mice killed at each chase time point ( $n=9$ ) were embedded in butyl-methyl methacrylate (BMMA), serially sectioned at  $2\mu\text{m}$ , and 3D reconstructions generated according to previous protocol (Parfitt *et al.*, 2012). Animals were treated according to the ARVO statement on the use of animals in vision research, and experiments were approved by the IACUC of the University of California, Irvine (P.I. Jester, protocol no. 2,011–3,002, approved 8 September 2011). After imaging GFP, sections were sequentially immunolabeled with CK6 (Abcam–Cambridge, UK, no. ab24646), SOX9 (Millipore–Billerica, MA, no. Ab5535),

and BLIMP1 (Abcam no.ab96479) and reimaged. Semi-automated alignment of serial montage images and 3D reconstruction was then carried out using Amira software (Visage Imaging, San Diego, CA). Finally, the total GFP<sup>+</sup> LRC count was quantified in three high-resolution 3D reconstructions of MGs and HF/SG at 28 (MG =  $25 \pm 4$ ; HF/SG =  $32 \pm 6$ ), 42 (MG =  $12 \pm 2$ ; HF/SG =  $29 \pm 7$ ), and 56-day (MG =  $9 \pm 3$ ; HF/SG =  $28 \pm 6$ ) chase through physical counting and ImageJ software (National Institutes of Health, <http://rsb.info.nih.gov/ij/>).

In Figure 1a, MG (encircled white) and HF/SG (encircled yellow) skin appendages of the eyelid are shown in histological section. After 28-day doxycycline chase, very few epithelial cells retain GFP in the H2B-GFP/K5tTA mouse MG (Figure 1b—red arrowhead) compared with the HF (Figure 1b—white arrowhead). In 3D (Figure 1c and Supplementary Movie S1 online), LRCs were observed at the transition between CK6<sup>+</sup> duct and acini epithelium of the MG. In the HF/SG 3D reconstruction (Figure 1D and Supplementary Movie S2 online), LRCs are restricted to the bulge region of the HF, and no LRCs were detected in the SG basal layer.

Quantification of total cells (Figure 2a) and LRCs (Figure 2b) expressing BLIMP1, SOX9, or CK6 in the MG and HF was performed on eyelids ( $n=3$ ) from mice euthanized at 56-day doxycycline chase. SOX9 and BLIMP1 were found to be expressed in the majority of MG and HF/SG epithelial cells, whereas LRCs occupy only a small

population in these tissues. There was a mean of  $9 \pm 3$  LRCs out of  $4356 \pm 497$  total cells per MG and a mean of  $28 \pm 6$  LRCs out of  $573 \pm 95$  total cells per HF (Figure 2a). LRCs in the MG were exclusively SOX9<sup>+</sup> and BLIMP1<sup>-</sup>, whereas HF LRCs exhibited a variable expression of SOX9 and BLIMP1 (Figure 2b). Slow-cycling MG cells express SOX9 as do terminally differentiated meibocytes (Figure 2c) and, in the HF, SOX9 is present in differentiated and quiescent cells (Figure 2d). In MGs, the putative sebocyte progenitor marker, BLIMP1, is absent in LRCs but present in differentiated epithelial cells (Figure 2e). BLIMP1 was found expressed in differentiated HF cells, bulge LRCs, and terminally differentiated sebocytes (Figure 2f). MG LRCs were localized to the ductal epithelium terminus where it transitions to basal acinar epithelium (Figure 2g) and infrequently express CK6, whereas HF LRCs are exclusively CK6<sup>-</sup> (Figure 2h).

Through immunofluorescence tomography, we have localized and quantified a slow-cycling population of the mouse MG found at the CK6<sup>+</sup> ductule that interconnects each acini with the central duct. We hypothesize that turnover of the MG epithelia may be directed from these quiescent epithelial cells. However, additional functional studies are required to validate the potency of these cells. In the HF, LRCs were restricted to the bulge zone and none were found in the SG basal layer in a total of 6 glands evaluated. After localizing LRCs, we immuno-stained for SOX9, a putative stem cell marker (Formeister *et al.*, 2009; Scott *et al.*, 2010) considered an essential adult stem cell gene (Nowak *et al.*, 2008). In the HF and MG of the eyelid, quiescent and differentiated cells express SOX9,

Abbreviations: HF, hair follicle; LRC, label-retaining cells; MG, meibomian glands; SG, sebaceous glands  
Accepted article preview online 14 November 2014; published online 18 December 2014

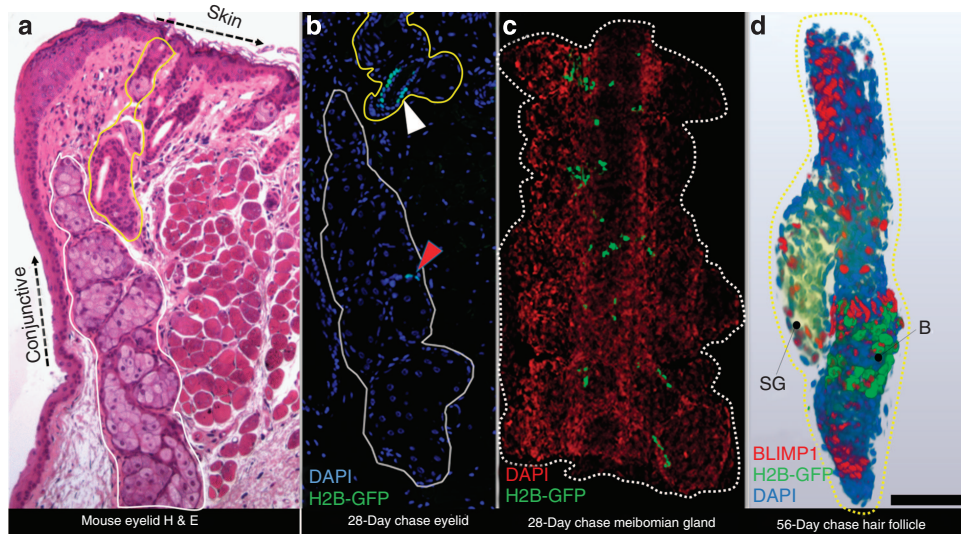


**Figure 1. Immunofluorescence tomography of the H2B-GFP/K5TtA mouse eyelid after doxycycline chase.** (a) Hematoxylin and eosin (H & E) staining of BMMA-embedded mouse eyelid showing the meibomian gland (encircled white) and hair follicle/sebaceous gland (encircled yellow). Both the meibomian gland (red arrowhead) and the hair follicle (white arrowhead) exhibit populations of slow-cycling epithelial cells after 28-day doxycycline chase. (c) In the meibomian gland, the label-retaining cells (LRCs) are located at the ductule or ductal epithelium terminus where the acinus forms. (d) BLIMP1 is expressed in differentiated hair follicle and sebaceous gland (SG) and is unlikely to be a marker of sebocyte progenitors. The hair follicle LRCs (green) are restricted to the bulge region (b) and are absent in the SG. Scale bar = 50  $\mu$ m.

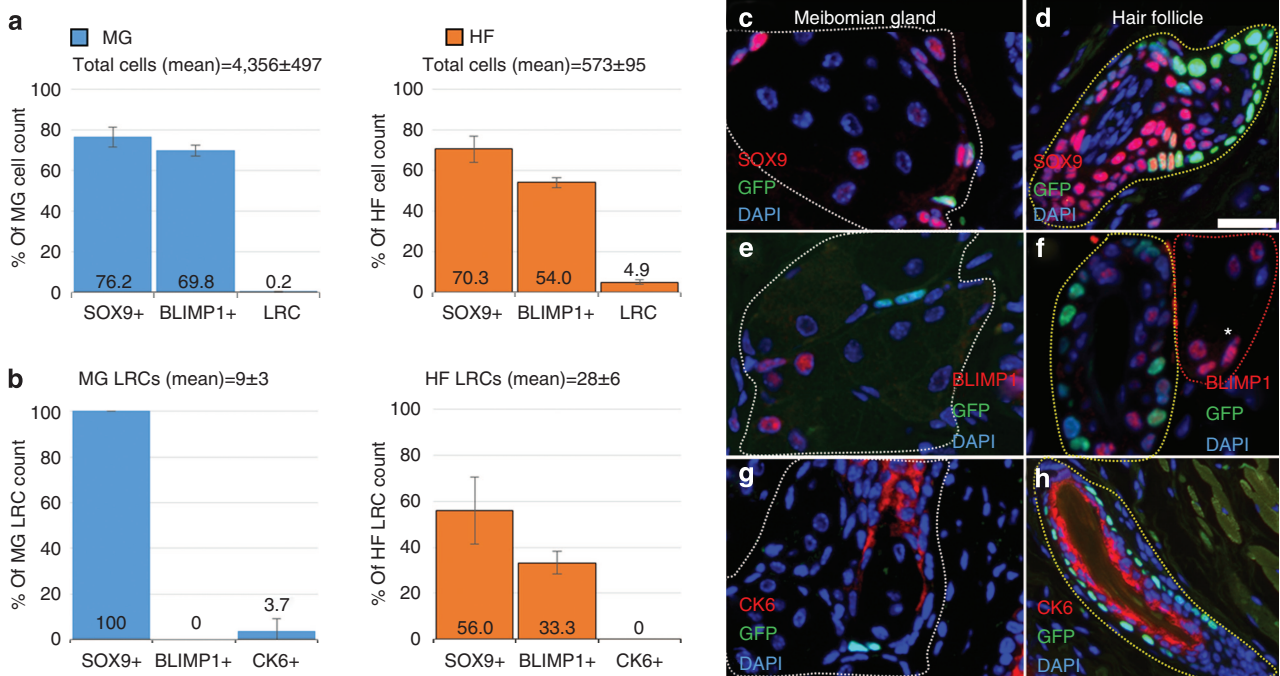


**Figure 2. Quantification of GFP<sup>+</sup> label-retaining cells (LRCs) and the expression of BLIMP1, SOX9, and CK6 in the meibomian gland and hair follicle/sebaceous gland after 56-day doxycycline chase.** (a) The average total cell and (b) LRCs that express either SOX9, BLIMP1, or CK6 in the meibomian gland (blue) or hair follicle (orange). (c–h) Immuno-staining of meibomian gland (c, e, and g—encircled white), hair follicle (d, f, and h—encircled yellow), and sebaceous gland (f\*—encircled red) showing co-localization of quiescent epithelial LRCs with (c and d) SOX9, (e and f) BLIMP1, and (g and h) CK6 in the H2B-GFP/K5TtA mouse after 56-day doxycycline chase. Scale bar = 50  $\mu$ m.

and therefore our data indicate that SOX9 is not a good marker of quiescent epithelial cells, although it still may

regulate stem cell quiescence as previously suggested (Nowak *et al.*, 2008; Kadaja *et al.*, 2014).

Previous research also suggests that the zinc-finger transcriptional repressor BLIMP1 is a marker of a unipotent

progenitor population that directs SG turnover and sebocyte differentiation (Horsley *et al.*, 2006). However, our high-resolution 3D data reveal that BLIMP1 is expressed throughout the HF in both quiescent and differentiated HF cells and sebocytes. Furthermore, BLIMP1<sup>+</sup> cells located near or in the SG were not found to be LRCs. This finding supports a more recent study, which found BLIMP1 in mature sebocytes, (Sellheyer and Krahl, 2010), raising important questions about the role of BLIMP1 and the true identity of sebocyte progenitor cells. The discovery of a slow-cycling population offers unprecedented insights into MG cell turnover and may shed light on MG age-related atrophy and dry eye disease.

#### CONFLICT OF INTEREST

The authors state no conflict of interest.

#### ACKNOWLEDGMENTS

This work was supported in part by NEI EY021510, the Skirball Program in Molecular Ophthalmology,

Research to Prevent Blindness, and Vistakon/ARVO Foundation.

**Geraint J. Parfitt<sup>1</sup>, Mikhail Geyfman<sup>1</sup>, Yilu Xie<sup>1</sup> and James V. Jester<sup>1</sup>**

<sup>1</sup>The Gavin Herbert Eye Institute, University of California, Irvine, Irvine, California, USA  
E-mail: JJester@uci.edu

#### SUPPLEMENTARY MATERIAL

Supplementary material is linked to the online version of the paper at <http://www.nature.com/jid>

#### REFERENCES

- Cotsarelis G, Cheng SZ, Dong G *et al.* (1989) Existence of slow-cycling limbal epithelial basal cells that can be preferentially stimulated to proliferate: implications on epithelial stem cells. *Cell* 57:201–9
- Formeister EJ, Sionas AL, Lorance DK *et al.* (2009) Distinct SOX9 levels differentially mark stem/progenitor populations and enteroendocrine cells of the small intestine epithelium. *Am J Physiol Gastrointest Liver Physiol* 296: G1108–18
- Horsley V, O'Carroll D, Tooze R *et al.* (2006) Blimp1 defines a progenitor population that governs cellular input to the sebaceous gland. *Cell* 126:597–609

- Kadaja M, Keyes BE, Lin M *et al.* (2014) SOX9: a stem cell transcriptional regulator of secreted niche signaling factors. *Genes Dev* 28:328–41
- Knop E, Knop N, Millar T *et al.* (2011) The international workshop on meibomian gland dysfunction: report of the subcommittee on anatomy, physiology, and pathophysiology of the meibomian gland. *Invest Ophthalmol Vis Sci* 52:1938–78
- Nowak JA, Polak L, Pasolli HA *et al.* (2008) Hair follicle stem cells are specified and function in early skin morphogenesis. *Cell Stem Cell* 3:33–43
- Parfitt GJ, Xie Y, Reid KM *et al.* (2012) A novel immunofluorescent computed tomography (ICT) method to localise and quantify multiple antigens in large tissue volumes at high resolution. *PLoS One* 7:e53245
- Pinto D, Clevers H (2005) Wnt, stem cells and cancer in the intestine. *Biol Cell* 97:185–96
- Scott CE, Wynn SL, Sesay A *et al.* (2010) SOX9 induces and maintains neural stem cells. *Nat Neurosci* 13:1181–9
- Sellheyer K, Krahl D (2010) Blimp-1: a marker of terminal differentiation but not of sebocytic progenitor cells. *J Cutan Pathol* 37:362–70
- Tumbar T, Guasch G, Greco V *et al.* (2004) Defining the epithelial stem cell niche in skin. *Science* 303:359–63

## A Single SNP Surrogate for Genotyping HLA-C\*06:02 in Diverse Populations

*Journal of Investigative Dermatology* (2015) 135, 1177–1180; doi:10.1038/jid.2014.517; published online 8 January 2015

#### TO THE EDITOR

Over forty-one genetic susceptibility loci of genome-wide significance ( $P < 5 \times 10^{-8}$ ) are known for psoriasis, a common complex genetic disease characterized by epidermal hyperproliferation and cutaneous inflammation. The most strongly associated of these loci maps to the *HLA-C* gene in the major histocompatibility complex (MHC) on chromosome 6p21.3 (Zhang *et al.*, 2009; Tsoi *et al.*, 2012). Recent fine-mapping studies have identified multiple independent association signals in the MHC, and the strongest signal is associated with HLA-C\*06:02 (previous designations: HLA-Cw6, HLA-Cw\*0602)

or single-nucleotide polymorphisms (SNPs) that are near-perfect surrogates for this allele (Feng *et al.*, 2009; Knight *et al.*, 2012; Das *et al.*, 2014; Okada *et al.*, 2014). HLA-C\*06:02 has been known to be psoriasis-associated since the 1970s, and most of the world populations that have been studied have shown strong evidence of association (Zhang *et al.*, 2009; Stuart *et al.*, 2010; Shaiq *et al.*, 2013; Okada *et al.*, 2014). Yet, it is difficult to perform a routine affordable laboratory test for the presence or absence of HLA-C\*06:02, because DNA-based testing is complicated both by the high degree of polymorphism of HLA-C (2375 alleles

encoding 1677 protein variations; July 2014 release of IMGT/HLA database; Robinson *et al.*, 2013) and by the sequence similarity of HLA-C\*06:02 to other HLA-C as well as HLA-A and HLA-B alleles. We previously used a seven-SNP genotyping system to unambiguously define HLA-C\*06:02 and several other HLA-C alleles (Nair *et al.*, 2006). Others have used allele-specific amplification followed by electrophoresis (Bunce *et al.*, 1995), PCR amplification followed by restriction enzyme digestion (Tazi Ahnini *et al.*, 1999), a combination of four surrogate SNPs that are amenable to Taqman genotyping (Nikamo and Stahle, 2012), and a three-SNP haplotype (rs1576-rs130076-rs2523619) known to be in strong linkage disequilibrium (LD) with HLA-C\*06:02 (Huffmeier *et al.*, 2009). Imputation of classical HLA alleles inclu-

Abbreviations: LD, linkage disequilibrium; MHC, major histocompatibility complex; SNP, single-nucleotide polymorphism

Accepted article preview online 10 December 2014; published online 8 January 2015